J. Fluid Mech. (1978), *vol.* 89, *part* 3, *pp.* 561–587
Printed in Great Britain

The turbulent mixing layer with an asymmetrical distribution of temperature

By CLAUDE BÉGUIER, LOUIS FULACHIER

Institut de Mécanique Statistique de la Turbulence,
Marseille, France

AND JAMES F. KEFFER

Department of Mechanical Engineering,
University of Toronto, Canada

(Received 14 March 1977 and in revised form 16 May 1978)

An experimental programme has been carried out to examine the spread of heat as a passive scalar contaminant in a turbulent shear flow. The situation involves a slightly heated two-dimensional jet expanding into a quiescent medium on one side and a uniform stream with velocity equal to that of the warm jet on the other. Thus the developed flow is a typical mixing layer with an asymmetric mean temperature profile superimposed on it. Measurements of the mean and fluctuating velocity and temperature fields show the existence of a region where the production of temperature fluctuations is negative. Spectral analysis in this zone indicates a separation of large and small wavenumber components of the cospectrum into two regimes. The sign of the high-frequency portion is consistent with gradient-transport concepts while the low-frequency component is of opposite sign. From this it is inferred that the large eddies are mainly responsible for the negative production. A mathematical model has been developed to describe the transport within this region.

1. Introduction

In turbulent shear flows it is generally accepted that the sum of the terms representing the production of turbulent kinetic energy is positive. The interpretation is that a continuous transfer of energy from the mean field to the turbulent motion takes place. This contributes to a state of equilibrium for the flow as the turbulent kinetic energy is passed to smaller and smaller scales, eventually being transformed into heat by the dissipation eddies.

It is not difficult to see, however, that in very localized regions of certain flows the sum of the production terms could become negative, without contradicting the fundamental laws of mechanics (Eskinazi & Erian 1969). There is experimental justification for this view. Erian & Eskinazi (1964), for a wall jet with a longitudinal pressure gradient, Béguier (1965*a*), for a wall jet with an external flow, Béguier (1969), for a two-dimensional asymmetric jet, and Palmer & Keffer (1972), for an asymmetric wake, have detected negative values of the production term which were of small but significant magnitude. Gosse & Schiestel (1975) also have confirmed the existence of a 'negative production' zone in a flow in an annulus by numerical predictions. The implication is that, locally, a transfer of kinetic energy from small to larger scales of

the turbulence is taking place, the latter conceivably being of the order of the width of the mean motion.

This phenomenon of 'energy reversal', a term coined by Eskinazi & Erian (1969), can be related directly to the large eddies of the flow from measurements of the spectral distribution of the Reynolds shear stress, as shown for the asymmetric plane jet (Béguier 1965*b*). It is presumably the influence of these large eddies upon the mean velocity profile which is responsible for the negative production. Although in each of the situations described above the profiles of the mean velocity were asymmetrical, this does not appear to be a necessary condition for the existence of the phenomenon. Indeed, experiments by Yule (1975) have shown that such energy reversal can occur in an axisymmetric flow when an axisymmetric magnetic body force is applied.

The negative values of the production in the cases cited above are related to the presence of a displacement between the zeros of the turbulent shear stress and the lateral gradient of the longitudinal mean velocity. It appears, however, that the asymmetry which is concomitant with this displacement is not a sufficient condition for negative production to exist. For example Mathieu & Tailland (1965) and Wilson (1974) found no evidence of negative production in a wall jet, although it must be pointed out that the total production term was close to zero in the region of displacement.

Although the interpretation and implications of negative production have been subject to some controversy, the observation of the displacement region between the zeros of the turbulent and mean shear stresses has been thoroughly documented for a number of asymmetric flows. In addition to those discussed above, there are the experiments of Eskinazi & Yeh (1956) on a curved channel, Gee & Bradshaw (1962) on a wall jet, Kjellström & Hedberg (1966) on an annular pipe flow and Hanjalić & Launder (1971) on a two-dimensional channel flow with walls of different roughness.

In the zone of displacement, the Reynolds stress is of opposite sign to the mean velocity gradient, and momentum transport by the turbulence cannot be described by conventional gradient modelling. Nevertheless, Launder (1968), Béguier (1969), Hinze (1970) and Hinze, Sonnenberg & Builtjes (1974) have, from theoretical considerations, proposed a modified relationship. The shear stress is decomposed into two parts: a gradient-type term which expresses the action of the small eddies and a term which, being proportional to the curvature of the mean velocity profile, essentially interprets the action of the large eddies. This can be thought of as an extension of the double-structure concept first proposed by Townsend (1956).

The experiments which have been carried out up to the present have been concerned only with the structure of the velocity field. However, the arguments presented above can, in principle, be extended to the case of any variable transported by the flow. In particular, for a flow with an asymmetric distribution of a passive scalar contaminant, one might reasonably expect to find a corresponding displacement between the positions where the transverse flux of the contaminant and the mean contaminant gradient are zero. In the displacement zone it would be necessary to examine the total production term for the contaminant fluctuations to see whether the net production is negative.

It is with this particular aim that we have undertaken the present investigation. The experimental configuration was designed to examine the properties of a dual

jet flow with unequal velocities (Béguier 1971), one of which was to be marked by a passive contaminant. It was assumed that the presence of negative production for the dynamic field which had been observed for this flow would precipitate a similar result for the contaminant field. As a first stage of this study, however, the velocities of the two jets were made equal. The experimental realization described in the present paper is therefore that of a simple mixing layer with a locally imposed distribution of a passive scalar contaminant spreading at the free edge.

2. Experimental methods

2.1. *Description of the apparatus*

The wind tunnel used in the present experiments is described by Béguier (1971). It consists of two independent air ducts, the upper having a variable-speed fan and two-stage contraction for the main jet and the other one of constant velocity to provide the external stream. A schematic diagram of the system is shown in figure 1. The height d of the exit slot of the main jet is 10 mm and its lateral width is 200 mm. The flow discharges into a channel consisting of two vertical parallel walls a distance of 200 mm apart, which constrains the mixing layer laterally. The intensity of turbulence at the exit for each stream is about 1 %. The two ducts were insulated to reduce the loss of heat to the surroundings and also to minimize the conduction heat transfer across the plate separating the two flows. In addition, this plate has been sharpened at the trailing edge to reduce the effect of the wake.

Upstream of the settling chamber for the jet flow a heating unit was installed. The system is composed of 12 grids, each of which contains eight cylindrical heating elements. The elements are constructed of an internal spiral of constant resistance wire, 0·14 mm in diameter, enclosed within a quartz tube with exterior diameter 5·74 mm. In order to permit adjustment of the temperature profile at the exit from the jet slot, provision was made for independent variation of the resistance of the heating elements, by means of a series of variacs and resistors.

2.2. *Measurement technique*

The longitudinal mean velocity was measured by means of a Pitot–static tube and constant-temperature hot wires. The mean temperature was determined with thermocouples fabricated from chromel–constantan wires. The exposed portion of the wire was aligned along an isotherm of the flow. The sensitivity of the thermocouples was of the order of 60 μV/°K. This permitted determination of the temperature to an accuracy of 0·2 °K.

The thermal fluctuations were determined with the aid of a cold wire (or resistance thermometer) and a constant-current anemometer. The cold wire was constructed of platinum with a diameter of 1 μm and a length of 0·3 mm and was heated by a constant current of 0·15 mA. This intensity was such that contamination by the fluctuating velocity field produced an error of less than 2 % of the r.m.s. value of the temperature fluctuations (Fulachier *et al.* 1974*a*). The constant-current bridge, designed and constructed at the I.M.S.T. by M. Astier, was compensated although the thermal inertia of the cold wire was very small, the time constant of the wire being about 50 μs.

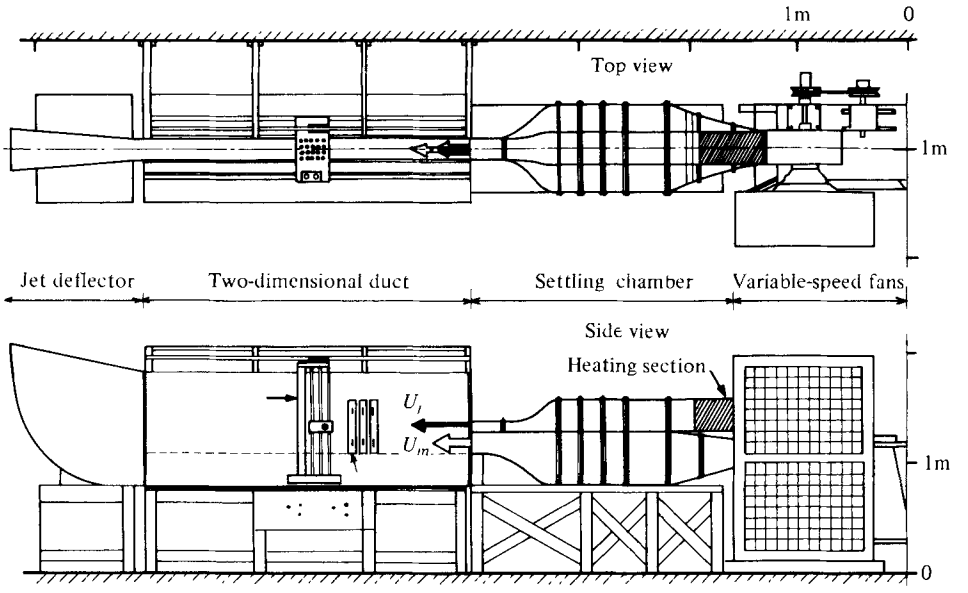

FIGURE 1. Definition sketch of apparatus.

For isothermal flow conditions the longitudinal velocity fluctuation u was measured with a tungsten–platinum hot wire 5 μm in diameter and 1 mm long. This was mounted normal to the mean flow, and the signal linearized and processed by a constant-temperature DISA anemometer system. The lateral fluctuation v, as well as the correlation between u and v, was determined using a conventional X-wire array with a separation distance of about 1 mm, a length of 1 mm and an enclosed angle of 90°. The signals from the X-wire were also linearized using a DISA system.

For heated flow conditions, the instantaneous values of u, v and θ were obtained simultaneously to evaluate the correlations between the velocity and thermal components. To effect this, a number of probes were developed. First, an arrangement using two normal wires in parallel, separated laterally, was constructed. This comprised a conventional, non-linearized hot wire together with a cold wire. The lateral separation distance between the two was found to be critical. In regions of intermittent flow, for wire separations of the order of 0·25 mm the hot wire influenced the cold-wire signal, yielding spurious temperature fluctuations. Too wide a separation would have increased the spatial resolution unacceptably, but eventually a distance of 0·50 mm was chosen as a suitable compromise. For purposes of later identification, this probe is designated P-2.

To obtain the lateral component of the velocity fluctuation in the heated flow, a second probe, designated X-D, was constructed. This consisted of an array of three wires: a conventional X-wire, as described above, with a cold wire located between them. The separation distance from the cold wire to each of the hot wires was 0·50 mm. For ease of calibration, a Pitot–static tube and thermocouple were mounted on the probe.

In each case, the hot wires will be sensitive to both the velocity and temperature fluctuations. However, with suitable analog processing of the signals from the two- or

three-wire probes the instantaneous fluctuations u and θ or u, v and θ can be obtained. Actually, a careful examination of the signals showed that the method used to separate u, v and θ did not eliminate completely the contamination of the u and v signals by θ. This was due to effects of nonlinearities and the frequency response of the system. As well, any multi-wire arrangement suffers from a spatial-resolution effect. It is only an approximation that the wires sense the same fluid particles in the velocity field, and thus the fluctuations in temperature and velocity will differ at the smallest scales.

To avoid some of these difficulties and in particular to ensure the accuracy of the v component with respect to θ, a new type of probe was used. The basic configuration had been developed earlier by Béguier *et al.* (1973) and has since been offered commercially by DISA. It consists of a parallel three-wire array (designated P-3) with a cold wire added to detect the thermal intensity fluctuations. This four-wire array is designated P-4.

2.3. *Spectral measurement technique*

From the fluctuations detected by the X-D probe, a spectral study of the flow has been made. The spectra F_u, F_v and F_w of the three components of the velocity fluctuations and the spectrum F_θ of the temperature fluctuations were measured with the aid of a spectral analyser system conceived by Dumas (1964). The range of frequencies extended from 1 to 6500 Hz. The output was proportional to nF_ξ, where F_ξ is the spectral density of the fluctuation quantity ξ normalized such that

$$\int_0^\infty F_\xi(n)\,dn = 1 \tag{2.1}$$

and n is the frequency. The bandwidth of the pass filter was equal to 5 % of the centre-frequency.

The cospectrum $E_{\theta v}(n)$, defined such that

$$\int_0^\infty E_{\theta v}(n)\,dn = -\frac{\overline{\theta v}}{(\Theta_m - \Theta_e)\,U_m} = \Phi, \tag{2.2}$$

was obtained from the difference of two spectra as follows:

$$E_{\theta v}(n) = a[\overline{(k_1 v_n + k_2 \theta_n)^2} - \overline{(k_1 v_n - k_2 \theta_n)^2}] = 4ak_1 k_2 \overline{\theta_n v_n}, \tag{2.3}$$

where ξ_n is the filtered value of ξ and a, k_1 and k_2 are the coefficients of amplification. It is not necessary to determine these independently since the overall coefficient $4ak_1 k_2$ can be obtained directly from the normalizing relationship (2.2).

For the special situation in the flow where the transport term Φ is zero, the above normalization method cannot be used and it is necessary to proceed in the following manner. The correlation coefficient $R_{\theta_n v_n}$ between the filtered fluctuations θ_n and v_n is determined directly from the four measured quantities contained in

$$R_{\theta_n v_n} = \frac{1}{4}\frac{\overline{(k_1 v_n + k_2 \theta_n)^2} - \overline{(k_1 v_n - k_2 \theta_n)^2}}{k_1 k_2 (\overline{v_n^2}\,\overline{\theta_n^2})^{\frac{1}{2}}} = \overline{\theta_n v_n}/(\overline{\theta_n^2}\,\overline{v_n^2})^{\frac{1}{2}}. \tag{2.4}$$

The spectra F_θ and F_v are then introduced to give the cospectrum:

$$E_{\theta v}(n) = \frac{(\overline{\theta^2}\,\overline{v^2})^{\frac{1}{2}}}{(\Theta_m - \Theta_e)\,U_m} R_{\theta_n v_n}(F_\theta F_v)^{\frac{1}{2}}. \tag{2.5}$$

It would be possible to determine $R_{\theta_n v_n}$ everywhere in the flow but, as can be seen above, this correlation coefficient needs four measurements, which may introduce many sources of error. Therefore we have determined the coefficient

$$r_{\theta_n v_n} = \frac{\overline{(k_1 v_n + k_2 \theta_n)^2} - \overline{(k_1 v_n - k_2 \theta_n)^2}}{\overline{(k_1 v_n + k_2 \theta_n)^2} + \overline{(k_1 v_n - k_2 \theta_n)^2}} = 2 \frac{k_1 k_2 \overline{\theta_n v_n}}{k_1^2 \overline{v_n^2} + k_2^2 \overline{\theta_n^2}}, \tag{2.6}$$

which needs only two measurements and is related to $R_{\theta_n v_n}$ by

$$r_{\theta_n v_n} = R_{\theta_n v_n} 2(F_\theta F_v)^{\frac{1}{2}}/(F_\theta + F_v), \tag{2.7}$$

the measurements being realized for $k_1/k_2 = (\overline{\theta^2}/\overline{v^2})^{\frac{1}{2}}$. We can see that $r_{\theta_n v_n}$ is not very different from the real correlation coefficient $R_{\theta_n v_n}$. It always has the same sign, being slightly smaller in magnitude. For example, $r_{\theta_n v_n} = 0{\cdot}96 R_{\theta_n v_n}$ for $F_\theta = 2F_v$. The two quantities eventually become equal in the case $F_\theta = F_v$.

3. Description of the flow

3.1. *Experimental realization*

A definition sketch of the flow showing the initial and fully developed profiles is given in figure 2. At the exit from the slot ($d = 10$ mm), the velocity U_j is equal to the velocity on the lower side U_m. The result is the formation of a simple mixing layer with the exception of the small wake formed by the dividing plate. The velocity scale for this mixing layer is taken as U_m. This was kept constant for all tests at $U_m \approx U_j = 15{\cdot}4\ \mathrm{m\,s^{-1}}$. The width scale l_0 was chosen as the distance between the points $y = y_{0{\cdot}5}$ and $y = y_{0{\cdot}9}$, where $U = 0{\cdot}5U_m$ and $U = 0{\cdot}9U_m$ respectively. The velocity variables were non-dimensionalized by these scales U_m and l_0.

The upper jet was heated, thus superimposing a distribution of temperature upon the velocity field. At the exit, the excess temperature $\Theta_{m0} - \Theta_e$ was 33 °K, where Θ_{m0} was the temperature of the jet fluid and Θ_e the ambient temperature. At subsequent positions downstream, the maximum temperature difference $\Theta_m - \Theta_e$, located at $y = y_m$, was taken as the mean temperature scale while the distance between the half maximum intensity points was taken to be $2l_\theta$. The scales for the thermal field were thus $\Theta_m - \Theta_e$ and l_θ, which were then used to non-dimensionalize the field variables (Béguier *et al.* 1975). Actually, the total pressures P_t at the exit for the two flows were equalized to produce the mixing layer and since the upper jet was heated we obtained $U_j = 1{\cdot}05U_m$ under normal conditions. The pressure and temperature profiles 2 mm downstream of the exit are shown in figure 3. The dividing plate creates an asymmetry within the temperature jump and a wake upon the velocity profile which practically disappear at the section $x/d = 20$.

The initial mean temperature scale $\Theta_{m0} - \Theta_e$ was determined from the following expression:

$$\rho_0 C_p U_j(\Theta_{m0} - \Theta_e) = \int_{-\infty}^{\infty} \rho C_p U(\Theta - \Theta_e)\, d(y/d), \tag{3.1}$$

where C_p is the specific heat at constant pressure. This expresses the excess of equivalent enthalpy per exit height d. $\Theta_{m0} - \Theta_e$ in fact differed by less than 0·4 °K from the maximum value $\Theta_m - \Theta_e$ of the temperature profile at the exit. Most of the measurements have been carried out at the section $x/d = 30$, where the maximum temperature

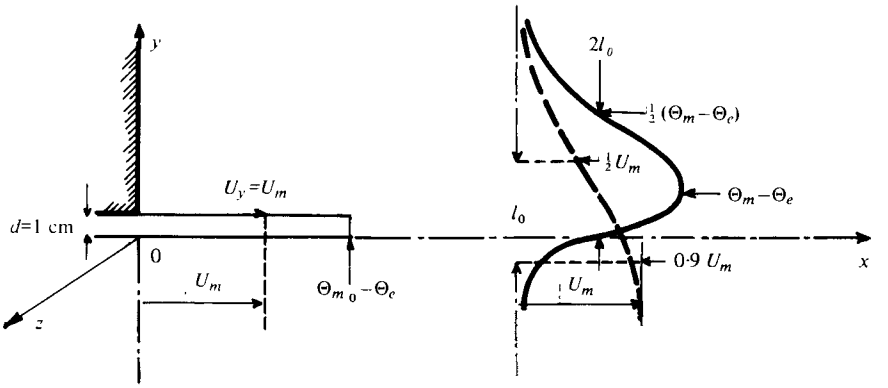

FIGURE 2. Definition sketch of flow field.

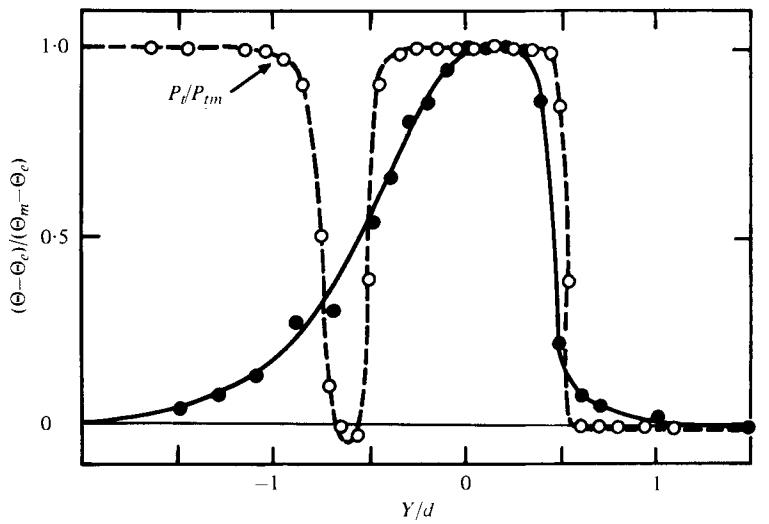

FIGURE 3. Initial conditions (P_t = total pressure).

difference was equal to 12 °K. The lateral profiles of mean velocity and temperature were measured at other stations and found to be uniform in the central portion of the channel. As well, the lateral correlations $\overline{uw}$ and $\overline{\theta w}$ for the velocity and thermal turbulent field were found to be substantially zero along the central plane $z = 0$. Thus the flow could be considered essentially two-dimensional.

3.2. *Governing equations*

For the developed flow shown in figure 2, one may write down the conservation equations which describe the coincident fields. The temperature difference is sufficiently small to assume that the buoyancy does not materially influence the motion, the absolute value of the Richardson number being of the order of 10^{-4}. As a consequence, heat can be regarded as a passive scalar contaminant for the fluctuations. The limitations to this approach have been discussed thoroughly by Favre (1965, 1975) and the order of magnitude of error for terms important to this present situation has been evaluated.

At the section $x/d = 30$, where $\Theta - \Theta_e \leqslant 12\,^{\circ}\mathrm{K}$, we can consider ρ as a constant through the mixing in the y direction. Under these conditions, $\overline{\rho U} = \rho U$ to an approximation of better than 0·5 %. However, for the lateral mean velocity it is necessary to take $\tilde{V}$, the velocity weighted by ρ, because (Verollet 1972)

$$\tilde{V} = \overline{\rho V}/\rho = V - \overline{\theta v}/\Theta. \tag{3.2}$$

The second term is not always negligible. For example, at the maximum value of $V \approx 0{\cdot}01 U_m$, it can produce an error of 4 %, and at the point in the mixing layer where $V = 0$, $\tilde{V} = -\overline{\theta v}/\Theta$ is different from zero. We have shown also that $\overline{\rho u v} = \rho \overline{u v}$ and $\overline{\rho \theta v} = \rho \overline{\theta v}$ to an approximation everywhere better than 1 %.

For the case of a two-dimensional mixing layer, where the viscous and conduction effects are negligible, the lateral spread is narrow enough so that the usual boundary-layer approximations can be employed. The equations of mean motion and of mean enthalpy can thus be written in the following way, taking account of the above considerations:

$$\frac{DU}{Dt} = U\frac{\partial U}{\partial x} + \tilde{V}\frac{\partial U}{\partial y} = -\frac{\partial}{\partial y}(\overline{uv}) - \frac{\partial}{\partial x}(\overline{u^2} - \overline{v^2}) \tag{3.3}$$

and

$$\frac{D\Theta}{Dt} = U\frac{\partial \Theta}{\partial x} + \tilde{V}\frac{\partial \Theta}{\partial y} = -\frac{\partial}{\partial y}(\overline{\theta v}) - \frac{\partial}{\partial x}(\overline{\theta u}). \tag{3.4}$$

The last terms of these equations are generally considered negligible by comparison with the others. In addition, the continuity equation is

$$\partial U/\partial x + \partial \tilde{V}/\partial y = 0. \tag{3.5}$$

One of our aims is to give special attention to the production terms for the velocity and temperature fluctuations. Considering first the dynamic field, we have the turbulent kinetic energy equation

$$\frac{D(\frac{1}{2}\overline{q^2})}{Dt} = U\frac{\partial(\frac{1}{2}\overline{q^2})}{\partial x} + \tilde{V}\frac{\partial(\frac{1}{2}\overline{q^2})}{\partial y} = \frac{\partial}{\partial y}\left[\overline{v\left(\frac{p}{\rho} + \frac{q^2}{2}\right)}\right] - \frac{\partial}{\partial x}\left[\overline{u\left(\frac{p}{\rho} + \frac{q^2}{2}\right)}\right] + \Pi - \epsilon, \tag{3.6}$$

where ϵ is the dissipation by viscosity, $\epsilon \simeq \nu(\overline{\partial u_i/\partial x_j})^2$, and the dynamic production terms are

$$\Pi = -\left(\overline{uv}\frac{\partial U}{\partial y} + (\overline{u^2} - \overline{v^2})\frac{\partial U}{\partial x}\right). \tag{3.7}$$

Π appears also, but with the opposite sign, in the mean kinetic energy equation

$$\frac{D(\frac{1}{2}U^2)}{Dt} = U\frac{\partial(\frac{1}{2}U^2)}{\partial x} + \tilde{V}\frac{\partial(\frac{1}{2}U^2)}{\partial y} = -\frac{\partial}{\partial y}(U\overline{uv}) - \frac{\partial}{\partial x}U(\overline{u^2} - \overline{v^2}) - \Pi. \tag{3.8}$$

In the general case, Π is positive and (3.6) and (3.8) show that an increase in the energy of the turbulent motion takes place at the expense of the energy of the mean field. Considering next the temperature field in an analogous way, the equation of temperature-fluctuation variance can be written as

$$\frac{D(\frac{1}{2}\overline{\theta^2})}{Dt} = U\frac{\partial(\frac{1}{2}\overline{\theta^2})}{\partial x} + \tilde{V}\frac{\partial(\frac{1}{2}\overline{\theta^2})}{\partial y} = -\frac{\partial(\frac{1}{2}\overline{\theta^2 v})}{\partial y} - \frac{\partial(\frac{1}{2}\overline{\theta^2 u})}{\partial x} + \Pi_\theta - \epsilon_\theta, \tag{3.9}$$

where ϵ_θ is the thermal dissipation or molecular smearing, $\epsilon_\theta \simeq \alpha\overline{(\partial\theta/\partial x_i)^2}$ (α being the thermal diffusivity), and the thermal production terms are

$$\Pi_\theta = -\left(\overline{\theta v}\frac{\partial\Theta}{\partial y} + \overline{\theta u}\frac{\partial\Theta}{\partial x}\right). \tag{3.10}$$

The corresponding mean equation is obtained by multiplying the enthalpy equation (3.4) by the mean temperature variation $\Theta - \Theta_e$:

$$\begin{aligned}\frac{D}{Dt}\left(\frac{(\Theta-\Theta_e)^2}{2}\right) &= U\frac{\partial}{\partial x}\left(\frac{(\Theta-\Theta_e)^2}{2}\right) + \tilde{V}\frac{\partial}{\partial y}\left(\frac{(\Theta-\Theta_e)^2}{2}\right)\\ &= -\frac{\partial}{\partial y}((\Theta-\Theta_e)\overline{\theta v}) - \frac{\partial}{\partial x}((\Theta-\Theta_e)\overline{\theta u}) - \Pi_\theta,\end{aligned} \tag{3.11}$$

in which Π_θ is subtracted from the terms on the right-hand side.

In the general case Π_θ is positive, and (3.9) shows that this produces an increase in the temperature fluctuation intensity, while (3.11) indicates that this represents a decrease in $(\Theta-\Theta_e)^2$. Since $\Theta-\Theta_e$ is positive in the present experiment, this corresponds to a decrease in the mean temperature variation. We emphasize here that heat is not considered as an energy quantity but as a passive scalar contaminant, i.e. a pollutant.

3.3. *Self-preserving expressions*

Although the above equations cannot be solved in close form, it is possible to predict the variation of certain important non-dimensional parameters. Following the method of Townsend (1956), a non-dimensional velocity $U/U_m = f(\eta)$ and, to a first approximation, a non-dimensional temperature $(\Theta-\Theta_e)/(\Theta_m-\Theta_e) = g(\eta_\theta)$ are defined, where $\eta = (y-y_{0.5})/l_0$ and $\eta_\theta = (y-y_m)/l_\theta$. It has been shown for a simple mixing layer [equation (3.3)] that $l_0 \sim (x-x_0)$ and U_m = constant. From the continuity equation (3.5) we obtain $\tilde{V}/U_m = h(\eta)$. Correspondingly, for the simplified enthalpy equation (3.4), we can assume for the lateral transport term $\overline{v\theta}/(\Theta_m-\Theta_e)U_m = k(\eta_\theta)$. When these quantities are substituted into the enthalpy equation (3.4), this becomes, in non-dimensional form,

$$fg\left[\frac{l_\theta}{\Theta_m-\Theta_e}\frac{d}{dx}(\Theta_m-\Theta_e)\right] - \eta_\theta fg'\frac{dl_\theta}{dx} - fg'\frac{dy_m}{dx} + hg' + k' = 0, \tag{3.12}$$

where $g' = \partial g/\partial\eta_\theta$ and $k' = \partial k/\partial\eta_\theta$. If $y_m \sim x - x_{0m}$ this has a self-similar solution

$$\frac{l_\theta}{d} \sim \frac{x-x_0'}{d}, \quad \frac{\Theta_m-\Theta_e}{\Theta_{m0}-\Theta_e} \sim \left[\frac{x-x_0'}{d}\right]^n, \tag{3.13}$$

where x_{0m} and x_0' are virtual origins for the velocity and thermal flows, not necessarily coincident with the physical origin at $x = 0$. An additional constraint on the system is that the enthalpy of the hot jet is conserved. In non-dimensional form this is

$$l_\theta U_m(\Theta_m-\Theta_e)\int_{-\infty}^{\infty} f(\eta)\,g(\eta_\theta)\,d\eta_\theta = \text{constant}. \tag{3.14}$$

If one assumes that η is proportional to η_θ, which appears reasonable in the case of an ideal experiment, the integral will be independent of x and

$$l_\theta(\Theta_m-\Theta_e) = \text{constant}. \tag{3.15}$$

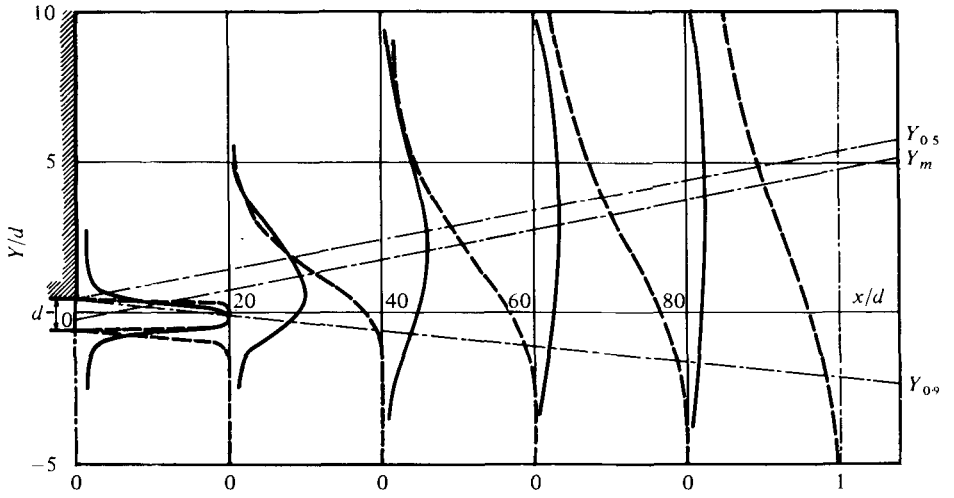

FIGURE 4. Development of mean flow. – – –, U/U_m; ——, $(\Theta-\Theta_e)/(\Theta_{m0}-\Theta_e)$.

From this it follows that the exponent in (3.13) is -1, so that the mean temperature scale varies inversely with x, as is found in a two-dimensional heated jet flow (Davies, Keffer & Baines 1975).

4. Results

4.1. *Mean flow development*

Figure 4 shows the experimental profiles of mean velocity and temperature as they evolve in the downstream direction. Preliminary measurements indicated that beyond the station $x/d = 30$ the heat had no discernible effect upon the velocity field. It should be noted that the positions of the half-maximum velocity, $y_{0.5}$, where $U/U_m = 0.5$, and the point $y_{0.90}$, where $U/U_m = 0.90$, are plotted in figure 4 and show a linear increase with x/d. Furthermore, the point of maximum temperature, y_m, where $(\Theta-\Theta_e)/(\Theta_m-\Theta_e) = 1$, increases linearly as well and is parallel to $y_{0.5}$. It is suspected that the magnitude of the difference between $y_{0.5}$ and y_m could be a function of the nozzle width d, although we have not explored this point further. In the ideal case, the initial temperature jump would be a Dirac delta-function, and $y_{0.5}$ and y_m would then be identical. Whether or not one would obtain an asymmetric temperature profile under this limiting condition is uncertain, however.

The set of profiles for the velocity field has been scaled by U_m and l_0, the results being presented in figure 5. It is clear that the velocity distributions are self-similar over the range of the experiment, and that the small wake produced by the dividing plate is of no significance beyond $x/d = 20$. It is remarked further that the mean velocity does not fall to zero at large values of η. This is an effect of the entrainment of ambient fluid by the moving stream and is consistent with previous results (Wygnanski & Fiedler 1970; Liepman & Laufer 1947). This figure shows also the intermittency factor γ (turbulent time/total time), which was obtained directly from numerous pictures of signals registered on a 'memory scope'. We note that the results for velocity and temperature fields are the same, as has been shown by Sunyach (1971)

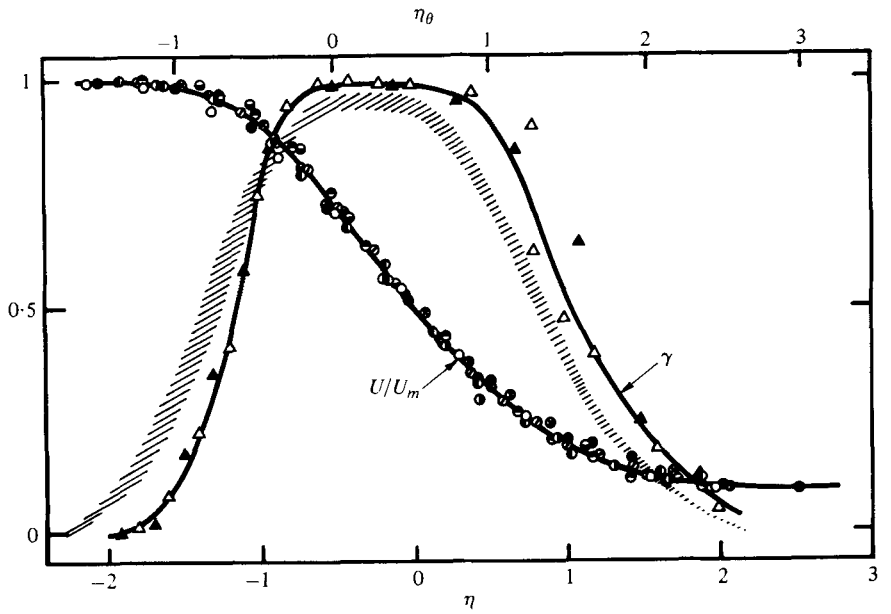

FIGURE 5. Self-similar profiles of mean velocity. x/d: ○, 20; ●, 30; ◑, 40; ◐, 50; ◓, 60; ◒, 70; ⊕, 80; ⊘, 100. $x/d = 30$: △, γ obtained from the velocity u; ▲, γ obtained from the temperature; ▨, γ obtained by Wygnanski & Fiedler (1970) in a mixing layer.

for the mixing layer of a plane jet and by Dumas, Fulachier & Arzoumanian (1972) for a boundary layer. The results are also comparable to those of Wygnanski & Fiedler (1970) for a mixing layer. The observed differences could be attributed to the initial conditions.

A similar presentation of the mean temperature field is given in figure 6. A number of comments can be made. The scatter of the results is slightly greater than for the velocity field. The profile is markedly asymmetric, the steeper gradient occurring on the high-velocity side. It is possible that the scatter represents a lack of complete self-similarity and that the asymmetric thermal profiles are undergoing a slow evolution towards some asymptotic state. If one characterizes the asymmetry by Δ, representing the abscissa η_θ of the middle of the segment bounded by the points where $(\Theta - \Theta_e)/(\Theta_m - \Theta_e) = 0{\cdot}5$, it is found that Δ increases, passes through a maximum of 0·28 at $x/d = 10$, then decreases steadily to 0·03 at the limit of the tests, $x/d = 80$. Nevertheless, one can assume that for all practical purposes the mean temperature field is essentially self-similar for the calculation of global parameters over the range measured.

Further information on the mean fields is given by the variation of the scales of the flow. Figure 7 shows the variation of the length scales for the velocity and thermal profiles with x/d. As predicted from the self-preserving analysis in § 3.3, these quantities increase linearly with x. One notes that the slopes are different for the two fields with $dl_0/dx > dl_\theta/dx$ and that the virtual origin for the temperature length scale is at $x/d = -7$, while that for the velocity field is at $x = 0$. The smaller slope of l_θ/d would appear to be anomalous. However, Davies *et al.* (1975) showed that the arbitrary 'conventional' length scales l_0 and l_θ are not true indications of the spread of the flow.

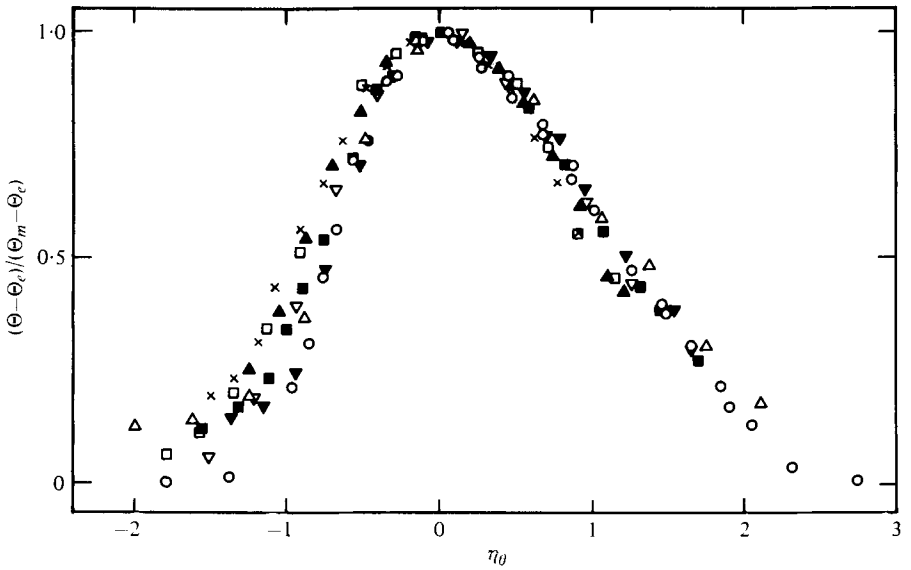

FIGURE 6. Self-similar profiles of mean temperature. x/d: △, 10; ▼, 20; ○, 30; ■, 40; ▽, 50; ▲, 60; □, 70; ×, 80.

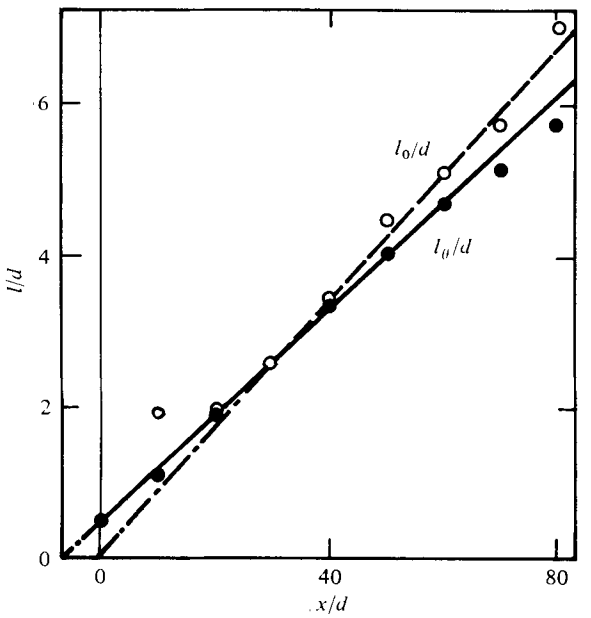

FIGURE 7. Variation of length scales for velocity (l_0/d) and temperature fields (l_θ/d).

Rather, a quantity which takes account of the effect of the intermittent nature of the flow and is not subject to differences in the behaviour of the temperature and velocity at the interface is required. Such a quantity is the half-intermittency point. This is in good agreement with the results shown in figure 5.

In the present experiment, the vorticity–temperature interfaces which exist at the two edges of the mixing layer are different. On the high-velocity side the spread of

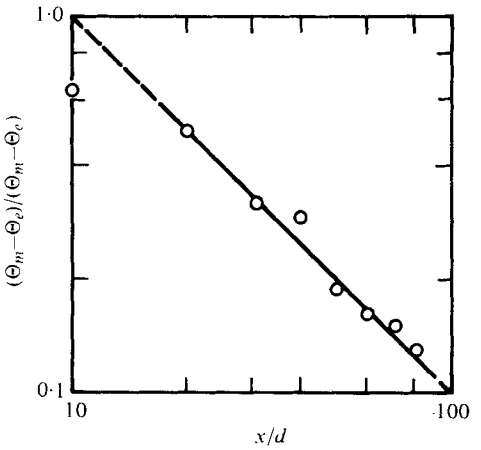

FIGURE 8. Variation of intensity of mean temperature.

turbulence is equivalent to a wake flow. Because of the background turbulence level in the high-velocity stream the transport of temperature is similar to the case of the pure thermal mixing layer of Keffer, Olsen & Kawall (1977). The low-velocity side, however, is equivalent to a hot jet (Davies *et al.* 1975). As a result careful definition and measurement of an appropriate length scale would be required to detail the exact nature of the net spread of the flow. This aspect is currently being investigated. Nevertheless, it is clear that, in a general way, the thermal length scale follows the self-preserving constraint.

The variation of the mean thermal intensity scale $(\Theta_m-\Theta_e)/(\Theta_{m0}-\Theta_e)$ is given in figure 8. This shows that the scale decreases with x/d in accordance with (3.13) and (3.15). It cannot be inferred from this, however, that the flow is completely self-preserving. Figures 7 and 8 indicate that the behaviour within the range tested is consistent with self-preservation, but more extensive tests would be required to reveal the final stage of evolution.

4.2. *Fluctuating components and correlations*

Measurements of the three components of the turbulent fluctuation intensities were made. The results for $x/d = 30$, non-dimensionalized by the mean velocity scale U_m and the length scale l_0, are presented in composite form in figure 9. The measurements of $(\overline{u^2})^{\frac{1}{2}}$ and $(\overline{v^2})^{\frac{1}{2}}$ were taken with a variety of probes (§ 2.2) for both heated and unheated flows. For the longitudinal component, it can be seen that there is no substantial effect due to the different probe arrangements or to heating, with the exception of the free edge of the layer, where the scatter in the results is slightly greater. In particular, the linearization of the signal has no marked influence upon the magnitude of this component. It should be noted that linearization could not be used in the technique which we employed in the present experiment for extracting simultaneous values of u, v and θ from the raw signals.

In contrast, the data for $(\overline{v^2})^{\frac{1}{2}}$ exhibit a dependence upon the linearization of the signal, the results being about 16 % lower for the linearized signal at the point of maximum intensity. Again, however, there is no discernible effect of the heating.

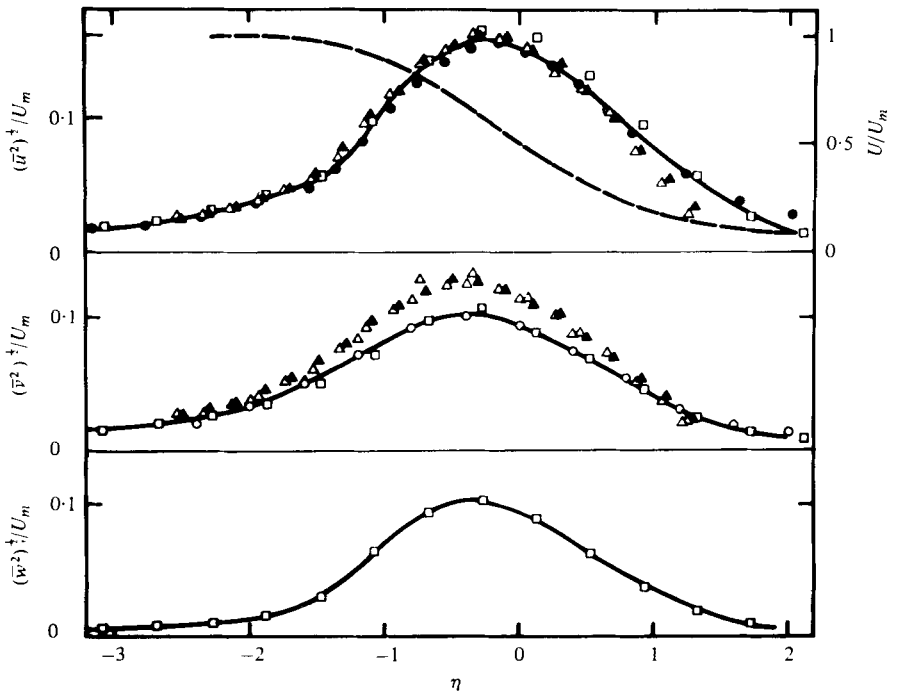

FIGURE 9. Profiles of velocity fluctuations intensities. Without heating: ●, linearized hot wire; □, linearized X-wire probe; △, X-D probe; ○, linearized X-D probe. With heating: ▲, X-D probe.

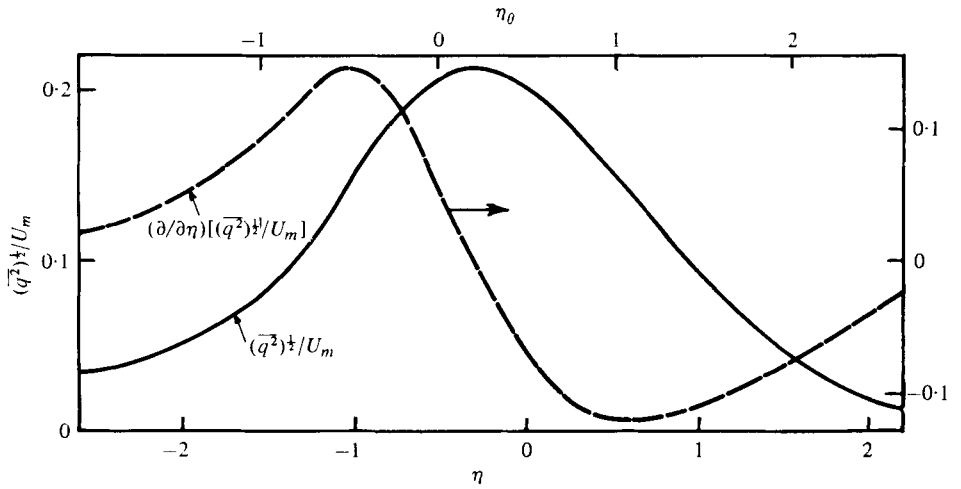

FIGURE 10. Turbulent kinetic energy profile.

The linearized $(\overline{w^2})^{\frac{1}{2}}$ results portray essentially the same form as the $(\overline{v^2})^{\frac{1}{2}}$ data with identical maximum values. These maximum values are of the same order as those measured by Wygnanski & Fiedler (1970) and Liepman & Laufer (1947).

From the results in figure 9, one can construct the distribution of the turbulent kinetic energy $\frac{1}{2}\overline{q^2} = \frac{1}{2}(\overline{u^2}+\overline{v^2}+\overline{w^2})$. This is shown in figure 10 along with the gradient

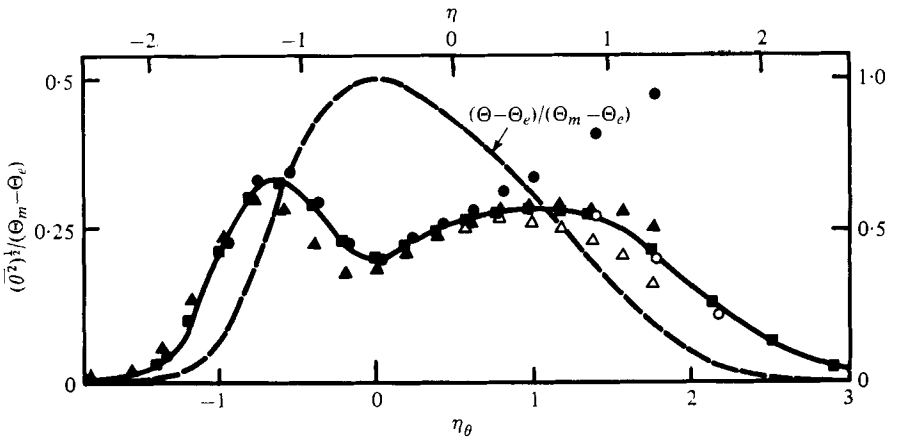

FIGURE 11. Profile of temperature fluctuation intensity. ■, single cold wire; △, X-D probe, X-wires not heated; ▲, X-D probe, X-wires heated; ○, P-2 probe, hot wire not heated; ●, P-2 probe, hot wire heated.

of $(\overline{q^2})^{\frac{1}{2}}$. It can be seen that the profile is slightly asymmetric with the steepest gradient on the high-velocity side of the mixing layer.

The thermal intensity fluctuations were taken at the same station, using both single-wire and multiple-wire probes. The results are shown in figure 11. A number of features are evident. The profile exhibits a minimum at the point where $\eta_\theta = 0$ and local maxima on each side of the centre, where $\partial(\Theta - \Theta_e)/\partial\eta_\theta$ itself is maximum. The magnitude of $(\overline{\theta^2})^{\frac{1}{2}}$ at these maxima is roughly proportional to the value of the gradient. Data on the high-velocity side of the mixing layer show little scatter. In contrast, a marked divergence occurs on the low-velocity side for results taken with the probe P-2 with two parallel wires. In this region the flow is highly intermittent and turbulent intensities are high. As a result, the wake from the hot wire will at times be convected across the cold wire, giving spurious thermal intensity fluctuations. The effect is eliminated when probe P-2 is operated with the hot wire turned off. A similar result is found for the X-D probe when the X-array is turned off.

With instantaneous values of u, v and θ known, the various correlations can be obtained. These are given in figure 12. It is evident that linearization of the signals has no effect upon the value of the correlation R_{uv}. The maximum value is equal to 0·51 and occurs slightly to the high-velocity side of $\eta = 0$. The correlations $R_{v\theta}$ and $R_{u\theta}$ can be expected to be in error for $\eta > 0{\cdot}5$ owing to the contamination of the cold wire by the wake of the hot wire in the highly intermittent zone. The dashed lines show the expected trend in this region.

Both $R_{v\theta}$ and $R_{u\theta}$ have similar forms: negative on the high-velocity side, then crossing to positive on the low-velocity side of the flow. These distributions are consistent with our physical understanding. Since $\overline{uv}$ will be positive everywhere, the signs of $\overline{u\theta}$ and $\overline{v\theta}$ will be identical, being either positive or negative depending upon the position in the flow. The dominant combinations ensure that for the high-velocity side of the flow we have ($u > 0$, $v > 0$, $\theta < 0$) or ($u < 0$, $v < 0$, $\theta > 0$) while for the low-velocity side ($u > 0$, $v > 0$, $\theta > 0$) or ($u < 0$, $v < 0$, $\theta < 0$). Conditional measurements, based on the signs of the fluctuations (Fulachier *et al.* 1974*b*), would have

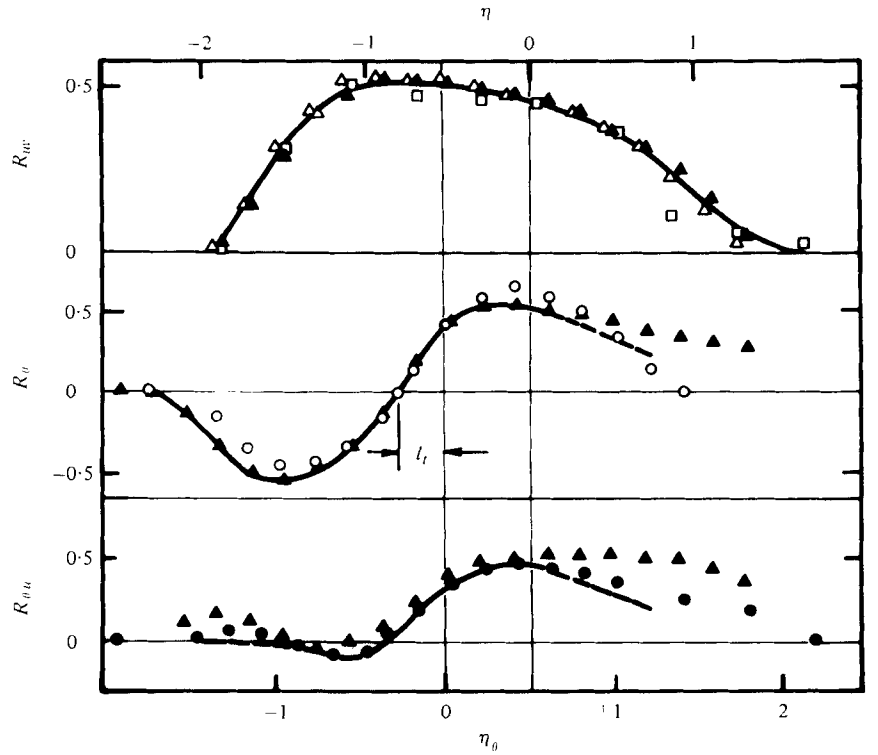

FIGURE 12. Velocity and temperature correlations. Without heating: □, linearized X-probe; △, X-D probe. With heating: ▲, X-D probe; ●, P-2 probe; ○, P-3 probe.

permitted us to determine the dominant mode in each region, but this was not attempted in the present experiment.

One important anomaly exists. As can be seen, a displacement occurs between the points where η_θ and $R_{v\theta}$ are zero. At this particular streamwise position, the displacement is significant: $|\Delta\eta_\theta| \simeq 0{\cdot}3$ or $\Delta y = 8$ mm. Clearly, in this zone the lateral enthalpy transport term cannot be proportional to the mean temperature gradient as is commonly supposed, since this would imply a negative coefficient of eddy heat transfer. One must thus search for a more effective model.

It has been pointed out that an analogous situation occurs in the velocity field of certain asymmetrical flows. Independently, Launder (1968), Béguier (1969) and Hinze (1970) described the motion in such zones by models which introduced a term in addition to the conventional gradient diffusion scheme, following the physical reasoning of Townsend (1956), who postulated a double structure for shear flows generally. The formulation within the displacement region is, following the idea of Townsend,

$$-\overline{uv} = \epsilon_m \partial U/\partial y - (\overline{uv})^*, \tag{4.1}$$

where ϵ_m is a turbulent eddy viscosity and $(\overline{uv})^*$ is the Reynolds stress corresponding to the actions of the big eddies. Since the derivative of the profile is quasi-linear near a velocity extremum, we can write, after Béguier (1969),

$$(\partial U/\partial y)_B = l_m(\partial^2 U/\partial y^2)_A$$

between the points A ($\partial U/\partial y = 0$) and B ($\overline{uv} = 0$), l_m being the length of the displacement zone. If we suppose that $(\overline{uv})^*$ is constant between A and B, which seems to be a good physical approximation, we then obtain from the conditions at the point B

$$-(\overline{uv})^*_{AB} = -\epsilon_m l_m (\partial^2 U/\partial y^2)_A,$$

and in this zone
$$-(\overline{uv})_{AB} = \epsilon_m (\partial U/\partial y)_{AB} - \epsilon_m l_m (\partial^2 U/\partial y^2)_A. \tag{4.2}$$

Otherwise, $\epsilon_m l_m$ can be related to the gradient of the turbulence intensity such that

$$\epsilon_m l_m = K_m l_0^3 (\partial(\overline{q^2})^{\frac{1}{2}}/\partial y)_A. \tag{4.3}$$

For the asymmetric plane jet the value of the dimensionless constant K_m was approximately $-0{\cdot}1$ (Béguier 1971) while l_0 was taken as the lateral width of the flow.

This point of view has been extended to the present thermal case. For the turbulent lateral flux at the temperature maximum (point A), we may write, as in the expression (4.1), for the displacement zone between A ($\partial\Theta/\partial y = 0$) and B ($\Phi = 0$)

$$(\overline{v\theta})^*_{AB} = k(\epsilon_\theta l_t)(\partial^2\Theta/\partial y^2)_A, \tag{4.4}$$

where ϵ_θ is the eddy diffusivity and l_t is the length of the displacement zone. The expression is multiplied by a coefficient k to take account of the nonlinearity of the temperature-profile derivative.

The total lateral turbulent flux can then be written in a dimensionless form:

$$-\frac{\overline{v\theta}}{(\Theta_m - \Theta_e)\, U_m} = \tilde{\epsilon}_\theta \left(\frac{\partial g}{\partial \eta_\theta} - k \frac{l_t}{l_\theta} \frac{\partial^2 g}{\partial \eta_\theta^2} \right), \tag{4.5}$$

where g and η_θ are defined in § 3.3 and $\tilde{\epsilon}_\theta = \epsilon_\theta / l_\theta U_m$. This last expression has been extended to the region located between the two inflexion points of the mean temperature profile, i.e. the major part of the centre-flow. The profile of $\tilde{\epsilon}_\theta$ at the section $x/d = 30$ is shown on figure 13. The constant k has been determined at the point B where $\Phi = 0$ and has been found to be equal to $0{\cdot}89$. We have plotted also the values of $\tilde{\epsilon}_{\theta B}$ (dashed line on the figure) and $\tilde{\epsilon}_m = \epsilon_m / l_0 U_m$, both obtained from the Boussinesq approximation. The values of $\tilde{\epsilon}_{\theta B}$ are negative in the displacement zone and are infinite near the temperature maximum. But $\tilde{\epsilon}_m$ and $\tilde{\epsilon}_\theta$ have the same order in magnitude and roughly the same variations. Finite values of the eddy diffusivity and of the turbulent Prandtl number ($Pr_t = \epsilon_m/\epsilon_\theta \approx 1$) are obtained in the displacement zone.

Actually, it would be necessary to consider in (4.5) the true mean turbulent temperature profile as measured by appropriate conditional sampling techniques (Davies *et al.* 1975), since the intermittency plays a different role on each side of the temperature maximum. Thus the given values of $\tilde{\epsilon}_\theta$ must be considered as rough indicative values. Nevertheless, following the procedure used in (4.3), we shall write

$$k\epsilon_\theta l_t = K_\theta l_\theta^3 \left(\frac{\partial}{\partial y} (\overline{q^2})^{\frac{1}{2}} \right)_A. \tag{4.6}$$

The value of the non-dimensional constant K_θ in this experiment has been found to be equal to $-0{\cdot}11$, and it can be seen that K_θ is not very different from the constant K_m determined for the dynamic case.

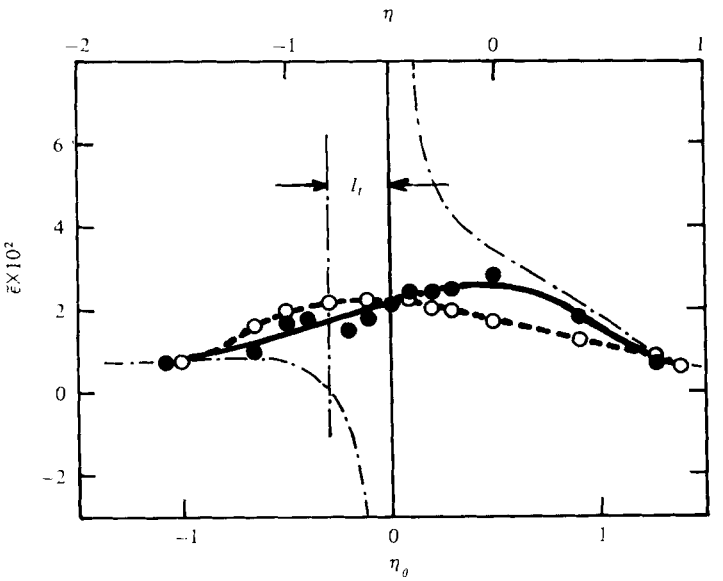

FIGURE 13. Eddy diffusivities and viscosity. —·—, $\tilde{\epsilon}_{\theta_B}$; – – –, $\tilde{\epsilon}_m$; ——, $\tilde{\epsilon}_\theta$.

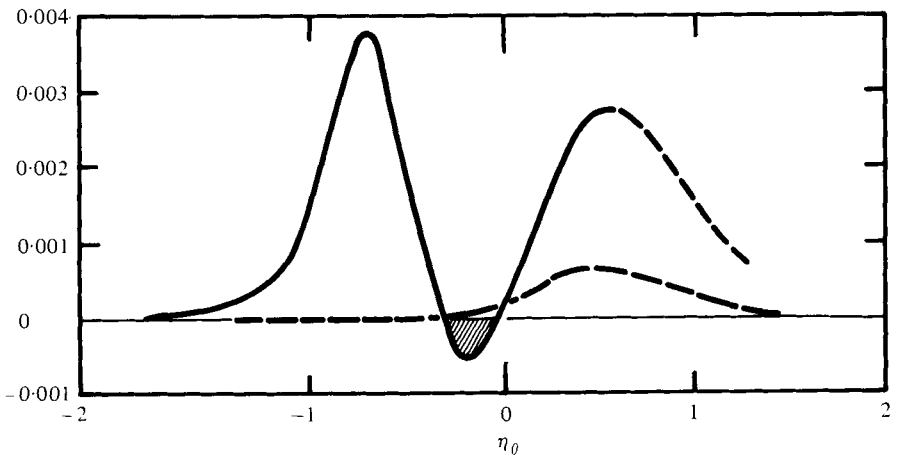

FIGURE 14. Production of temperature fluctuation intensity.

——, $\Pi_\theta = -[d/(\Theta_m-\Theta_e)^2 U_m][\overline{\theta v}(\partial\Theta/\partial y)+\overline{\theta u}(\partial\Theta/\partial x)]$;

– – –, $\Pi_{\theta_x} = -[d/(\Theta_m-\Theta_e)^2 U_m][\overline{\theta u}(\partial\Theta/\partial x)]$.

4.3. *Turbulent production*

The term representing the production of thermal fluctuations, $\Pi_\theta = -\overline{u_i\theta}\partial\Theta/\partial x_i$, is plotted in figure 14 as a function of η_θ. This is seen to become negative for

$$-0{\cdot}3 \leqslant \eta_\theta \leqslant 0.$$

This region is situated between the zeros of $\partial\Theta/\partial y$ and $\overline{v\theta}$. Furthermore, the magnitude of the negative portion is significant, representing 13% of the maximum positive value of the transport term. Further experiments made with different initial values

of the temperature and velocity confirmed the results, although the data are not presented here. In all cases the total production was determined from direct measured values rather than by assuming functional forms for the profiles of correlations and velocity gradients.

The situation above is analogous to the dynamic case, where $\Pi = -\overline{u_i u_j}\,\partial U_i/\partial x_j$, which is the total production of turbulent kinetic energy, has been observed to become negative in certain local regions of the flow. There is an essential difference between the two cases, however. In a velocity field, a passive scalar contaminant cannot affect the production of kinetic energy of the turbulence, whereas in the contaminant field the phenomenon of negative production is a consequence of the diffusive nature of the turbulence. In a real sense, the movement of the thermal quantities reflects the behaviour of the dynamic turbulent eddy structure. We comment further upon this in the next section.

4.4. *Spectral interpretation*

Spectral measurements were made in the region of negative production to help provide some understanding of the physical mechanisms which are responsible for the phenomenon. Figure 15 presents the spectra of the three components u, v and w of the velocity fluctuations as functions of the frequency n, taken at the position $\eta_\theta = -0{\cdot}314$ where the non-dimensional lateral transport of enthalpy

$$\Phi = -\overline{\theta v}/(\Theta_m - \Theta_e)\,U_m$$

is zero.

The spectral values have been normalized according to (2.8). Included is the spectrum of v calculated from the spectrum of u using the isotropic relationship

$$F_v(\text{iso.}) = \tfrac{1}{2}(F_u - n\,\partial F_u/\partial n). \tag{4.7}$$

It can be seen that the flow is effectively isotropic for frequencies beyond 400 Hz. This corresponds to $K_1 \gtrsim 1/\lambda_f$, where $K_1 = 2\pi n/U$ and

$$\lambda_f = U\left[2\overline{u^2}\Big/\overline{\left(\frac{\partial u}{\partial t}\right)^2}\right]^{\frac{1}{2}}$$

is the longitudinal microscale of the turbulence, which has the approximate value 5 mm in the present case. The turbulent Reynolds number $R_\lambda = (\overline{u^2})^{\frac{1}{2}}\lambda_f/\nu$ was about 600, high enough so that, between 80 and 800 Hz, approximately, the spectrum for u obeyed the $-\frac{5}{3}$-power law.

As the frequency approaches zero, it is found, like the results for the velocity mixing layer of Wygnanski & Fiedler (1970), that

$$\overline{v^2}F_v \approx \overline{w^2}F_w, \quad \overline{u^2}F_u \approx 5\overline{v^2}F_v.$$

This permits a determination of the macroscale ratio for the turbulence according to the ratio $L_u/L_v \approx 5\overline{v^2}/\overline{u^2}$, since $L_\xi = \frac{1}{4}UF_\xi(n \to 0)$.

Figure 16 shows the results of applying the analogy of Fulachier & Dumas (1976) between the temperature and the spectrum of the total velocity, the latter being given by

$$Q = (\overline{u^2}F_u + \overline{v^2}F_v + \overline{w^2}F_w)/\overline{q^2}. \tag{4.8}$$

The results here have been obtained for a situation where the velocity and temperature fields are significantly different. Nevertheless, it can be seen that the two spectra are closely matched. The small differences which exist can be attributed mainly to

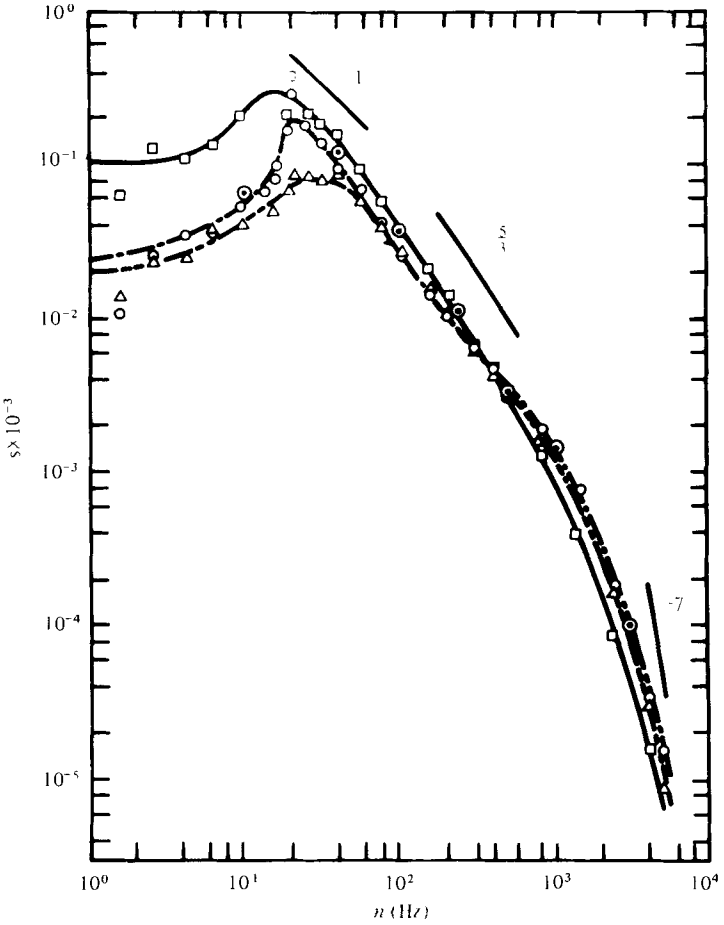

FIGURE 15. Spectra of turbulent fluctuation intensities of the velocity components. □, $(\overline{u^2}/U_m^2)F_u$; ○, $(\overline{v^2}/U_m^2)F_v$; △, $(\overline{w^2}/U_m^2)F_w$; ○, $(\overline{v^2}/U_m^2)F_v$(iso.).

experimental error. The existence of a peak is evident at 22 Hz. This results from a resonance of the fan used to produce the jet flow. The effect on the spectra is very localized, however, and is virtually undetectable in the conventional log–log representation. From these preliminary spectral results it can be seen that, despite the rather unusual initial conditions, the spectra of the velocity and especially the temperature fluctuations behave normally.

In order to investigate the structure of the flow in the region of negative production, the cospectra $E_{\theta v}$ of the lateral transport term, suitably normalized as in (2.9), are presented. Figure 17 shows the evolution of $nE_{\theta v}$ across the flow. In particular, the upper diagram, figure 17(a), portrays the cospectrum for the point where negative production is a maximum, $\eta_\theta = 0{\cdot}157$. At this position

$$\frac{\partial}{\partial \eta_\theta}\left(\frac{\Theta-\Theta_e}{\Theta_m-\Theta_e}\right) = 0{\cdot}27, \quad \Phi = -0{\cdot}0060.$$

It can be seen from these results that the regions with opposite sign effectively define the contributions from the low- and high-frequency components of the motion. The

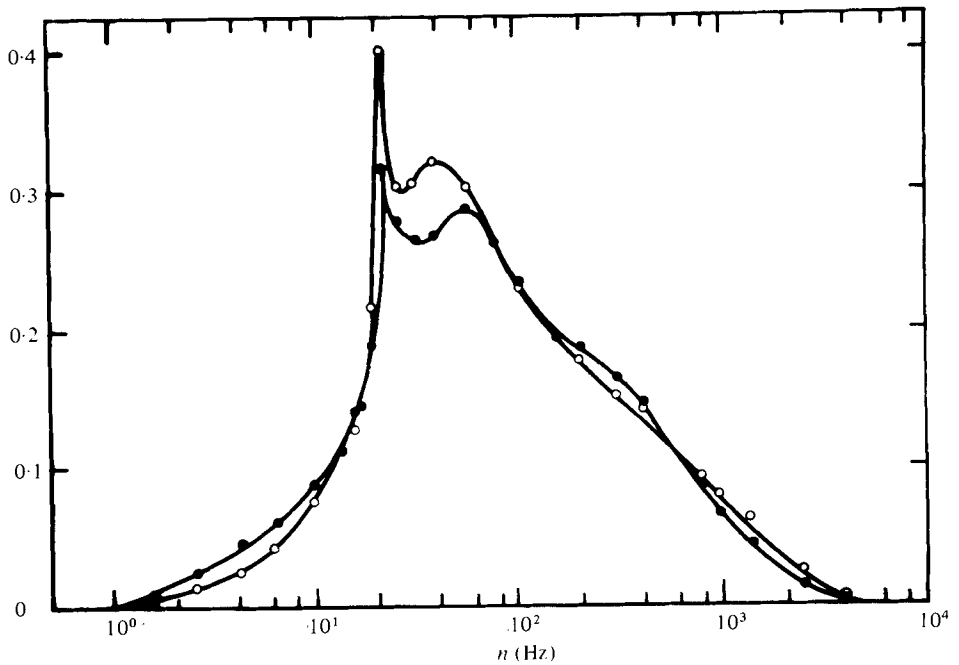

FIGURE 16. Spectral analogy between temperature and velocity. ●, nF_θ; ○, nQ.

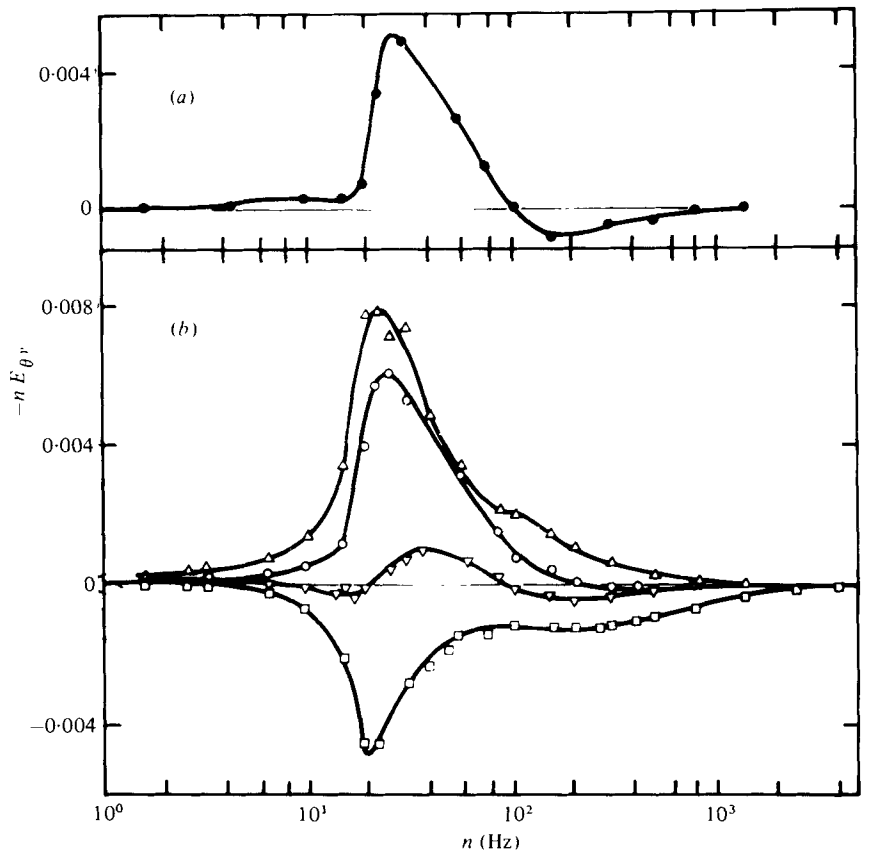

FIGURE 17. Cospectra of velocity and temperature. ●, $\eta_\theta = -0{\cdot}157$; △, $\eta_\theta = 0{\cdot}579$; ○, $\eta_\theta = 0$; ▽, $\eta_\theta = -0{\cdot}314$ ($\Phi = 0$); □, $\eta_\theta = -0{\cdot}927$.

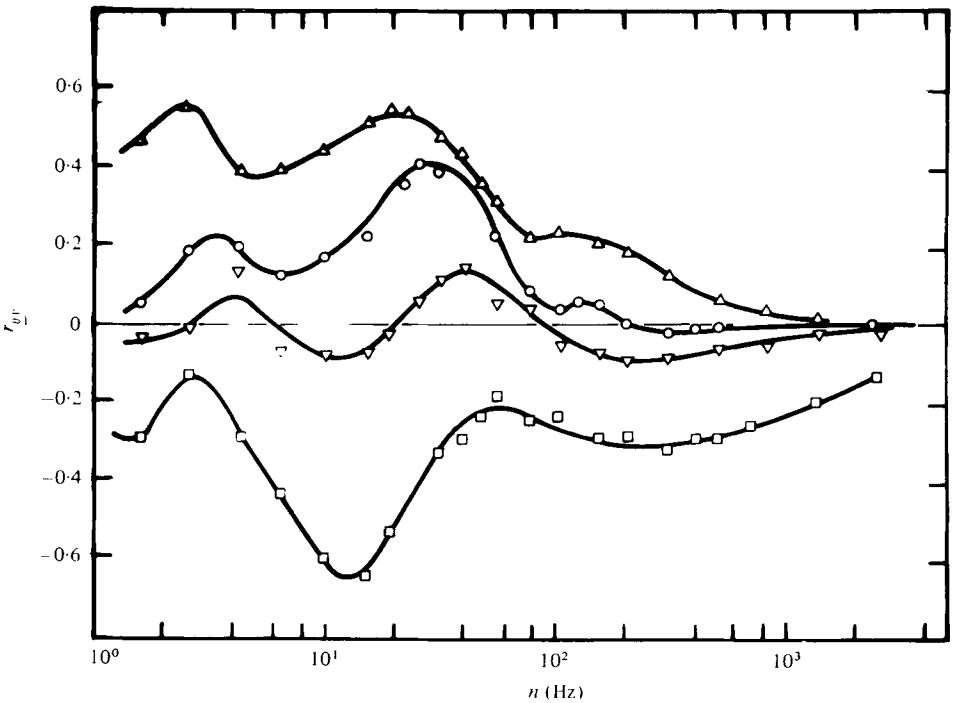

FIGURE 18. Spectral pseudo-correlation coefficient. △, $\eta_\theta = 0{\cdot}579$; ○, $\eta_\theta = 0$; ▽, $\eta_\theta(\Phi = 0) = -0{\cdot}314$; □, $\eta_\theta = -0{\cdot}927$.

change in sign occurs at about 100 Hz, which corresponds to $K_1 \approx 1/L_u$. The portion of $E_{\theta v}$ corresponding to the highest frequencies is of the same sign as the mean temperature gradient whereas the lowest frequencies produce a transport of opposite sign to that of the gradient. It can thus be inferred that the low-frequency components, which are related to the largest eddies of the flow, are the main mechanism for the negative production of temperature fluctuation intensity. The presence of two distinct regions in the cospectrum, one negative and the other positive, rather than a single positive zone of equal net area, tends to support the double-structure concept of Townsend (1956) for the transport. The above results are similar to those found for the velocity field in an asymmetric plane jet (Béguier 1969) or in a fully developed asymmetric flow in a plane channel (Hanjalić & Launder 1971).

An examination of the curve for which

$$\eta_\theta = 0{\cdot}579, \quad \Phi = -0{\cdot}0126, \quad \frac{\partial}{\partial \eta_\theta}\left(\frac{\Theta - \Theta_e}{\Theta_m - \Theta_e}\right) = -0{\cdot}47,$$

and the curve for which

$$\eta_\theta = -0{\cdot}927, \quad \Phi = 0{\cdot}0073, \quad \frac{\partial}{\partial \eta_\theta}\left(\frac{\Theta - \Theta_e}{\Theta_m - \Theta_e}\right) = 0{\cdot}72,$$

in figure 17(*b*), taken outside the region of negative production, where the gradients are approximately linear, shows a tendency towards a bimodal shape. Although there is no distinct gap in these cospectra, this behaviour may be taken as further evidence of the double structure. The situation for the point of maximum temperature

($\eta_\theta = 0, \Phi = -0{\cdot}0088$), where the gradient is zero, is consistent with the above results. The contribution to the covariance from the smallest eddies is effectively zero, which confirms that these higher-frequency components are directly related to the gradient of mean temperature.

Finally, the results for the position where the transport terms Φ are zero, for which

$$\eta_\theta = -0{\cdot}314, \quad \frac{\partial}{\partial \eta_\theta}\left(\frac{\Theta - \Theta_e}{\Theta_m - \Theta_e}\right) = 0{\cdot}59,$$

are presented. It can be seen that the contribution from each of the two populations is clearly evident and, as would be expected for zero transport, the areas corresponding to the high- and low-frequency components are equal.

Additional measurements have been made to confirm the interpretation given above. The variation of the pseudo-spectra correlation coefficient $r_{\theta_n v_n}$ was evaluated for the five lateral locations across the flow. These results, shown in figure 18, are seen to be generally consistent with the data in figure 17. There is a change in the sign of the correlation term for $\Phi = 0$ (curve 3) in the region beyond approximately 50 Hz, which delimits the contribution from the low and high frequencies.

Furthermore, the structure of the flow, as marked by the temperature, while similar to that in figure 17, shows in addition a complex evolution of the large eddies as the flow is traversed laterally. Even though this portion of the spectrum could be affected by the parasitic influence of the fan (figure 16) there appears to be a consistent dependence of the low-frequency structure upon the sign of the mean temperature gradient. This gives a maximum of $|r_{\theta_n v_n}|$ on one side of the mean temperature profile and a minimum on the other side at approximately the same wavenumber. The slight shift can be attributed primarily to the difference in the convection velocities on the two sides.

5. Summary and discussion

It would seem appropriate at this point to review some of the features which characterize the anomalous behaviour which occurs when the mean velocity field is asymmetric. Experimental evidence shows that a displacement between the points where the viscous and turbulent shear stresses are zero can occur, these points defining the limits of a zone of opposing shear. The signs of the stresses are thus different and the principal term in the expression for production of turbulent kinetic energy, i.e. $-\overline{uv}\,\partial U/\partial y$, becomes negative. Furthermore, if in this zone the other components of Π are either small in comparison with the normally dominant term or of the same sign, then an energy reversal results within this region of the flow. The implication must therefore be that there is a transfer of energy from the turbulent kinetic energy equation to the mean motion kinetic energy equation and even *perhaps* a gain by the mean motion at the expense of the turbulence (Eskinazi & Erian 1969). This last point of view is subject to certain controversy (Hinze 1970).

The physical explanation of the energy reversal is intimately related to that of the observed experimental displacement. Gee & Bradshaw (1962) suggest that, for the wall jet, 'packets of fluid having negative shear stress will frequently penetrate into the wall layer', where the mean velocity gradient is positive, and thus give a total contribution to the shear stress which is opposite in sign to that produced by the

mean gradient. This has been confirmed by spectral measurements in an asymmetrical plane jet by Béguier (1969). Generally then it can be inferred that the zone of displacement results from an asymmetrical lateral diffusion of large eddies from one side of the extremum of the mean velocity profile to the other. In the displacement region these large eddies would impose the sign of the shear stress which they had carried with them. The asymmetrical diffusion process would depend on the lateral gradient of kinetic energy of turbulence which exists at the extremum and which functions in a manner similar to a pressure gradient. As for the energy reversal, these big eddies would be able to transfer part of their mechanical energy to the mean motion perhaps by interaction between the mean velocity gradient and their instantaneous rotational vector. This phenomenon certainly exists on an instantaneous basis in symmetrical situations in the region around a velocity extremum, but the condition of symmetry invokes equal diffusion of large eddies from one side to the other. In fact, if one were able to inspect the energy exchange process on an instantaneous basis, as has been suggested by Brodkey *et al.* (1973), it would appear likely that temporary energy reversals could occur within all localized regions of the flow: a simple result of the fluctuating nature of the turbulent field. In ordinary flow situations then, time averaging eliminates this temporal fluctuation and the mean spectrum shows a steady transfer of kinetic energy from smaller to higher wavenumbers through to the viscous sink. From this point of view, the problem of energy reversal existing around a velocity extremum under asymmetrical conditions appears essentially to be a statistical one (J. Mathieu, private communication).

One further distinction can be made. When initial conditions are responsible for the asymmetry of the profile and subsequent creation of the zone of opposing shear, it is natural to examine the development of the motion. From our understanding of free turbulent shear flows it would appear likely that, regardless of the peculiarities of the origin, the motion should approach, if only asymptotically, a symmetric, self-similar or, depending upon the constraints, self-preserving form. This was shown to be the case for the wake generated by a double cylinder of Palmer & Keffer (1972). By approximately 80 diameters of development, the flow had become independent of the generating conditions and could be treated as a classic two-dimensional turbulent wake. It was noted above (4.1) that in our present flow the variation of the parameter Δ suggests evolution of the thermal field. With wall-bounded, asymmetric flows, however, such as the wall jets of Erian & Eskinazi (1964) and Béguier (1971) and the roughened conduit of Hanjalić & Launder (1971) to mention a few, the disturbing mechanism responsible for the asymmetry remains and the zone of opposing shear continues to be an essential feature of the motion.

It is interesting to examine the situation at very low wavenumbers. The largest scales of the turbulence will be of the same order, initially, as that of the apparatus used to generate the turbulent flow. As the flow develops and grows laterally, this scale must increase, i.e. the size of the largest eddies, at least in an unrestricted free shear flow, must continue to grow in the streamwise direction. If these large eddies come from the coalescence of small eddies, as the experiments on vortex pairing by Winant & Browand (1974) and Brown & Roshko (1974) suggest, then this phenomenon of a reverse cascade is asymptotically a true energy reversal. If the energy comes from the mean field, then the situation is described by conventional arguments.

Considering the present experiment, we can describe in an analogous manner an

equivalent phenomenon of energy reversal in a scalar contaminant field. In this case, the mean velocity profile is that obtained in a classical mixing layer, and a superimposed jump in heat at the free edge gives an asymmetrical mean temperature profile. We recall here that the buoyancy effects are negligible. The experimental results show that a displacement occurs between the points where the turbulent lateral heat flux and the mean temperature gradient are zero. (Deardorff (1966) has found a similar situation in the lower atmosphere but in this case the effect was caused by buoyancy.)

Pursuing the analogy, the production term for the thermal fluctuations normally represents the net transfer of contaminant intensity from the mean to the fluctuating field. This is equivalent to the cascade of turbulent kinetic energy. The scalar quantity in this case, however, is being convected by, and is thus intimately associated with, the velocity field. A progression through to successively higher wavenumbers thus implies the breakdown of the temperature structure until, in the limit, conduction processes cause a smoothing of the contaminant field, i.e. $\overline{\theta^2}$ is ultimately eliminated by the molecular sink. The existence in the displacement zone of negative values of Π_θ implies that negative production of $\overline{\theta^2}$ can take place in a classical turbulent flow, viz. the mixing layer. These values are more significant than in the dynamic case, since they reach 13 % of the maximum positive values, while in the dynamic case they have not been observed to exceed 5 %. The general results of our present experiments have been confirmed by experiments carried out by Charnay & Schon (private communication) upon the boundary layer of a plate heated from the leading edge and cooled at a point downstream. In this case buoyancy effects were also negligible.

We can conclude that there is a certain analogy between the negative thermal production in the present experiment and the dynamic energy reversal in asymmetrical flows. The cospectra measurements of the lateral turbulent heat flux show that it is the large eddies which are responsible for the negative thermal production. This cannot be regarded as a special situation, however. In a sense we are merely using the behaviour of the temperature field here to infer some features of the velocity field. The dynamic motion creates an asymmetrical transport of the big eddies which is stronger in the direction from low- to high-velocity regions. The direction of this diffusion is, in our case, of opposite sign to the lateral gradient of the turbulence intensity at the maximum temperature.

It has been shown for our situation that, for the lateral heat flux, an extension of the Reynolds-stress expression can take into account the countergradient turbulent heat fluxes by introducing a turbulent bimodal structure. The mechanics of this type of modelling can be seen by reference to simple mixing-length arguments. Figure 19 shows two situations.

(*a*) The transfer process within a constant gradient zone.

(*b*) The asymmetric situation as it occurs in the present experiment.

In case (*a*), the lateral heat flux can be explained from particle exchanges between the two planes 1 and 2 ($u^-\theta^+$ and $u^+\theta^-$), which contribute to the erosion of the mean temperature profile. In the asymmetrical condition it is necessary to modify the reasoning for the 'displacement zone' between planes 1 and 2. Although the usual lateral heat flux exists for the small-scale structure, as spectral measurements show, the dominant lateral heat flux in this zone, which is opposite to the mean gradient,

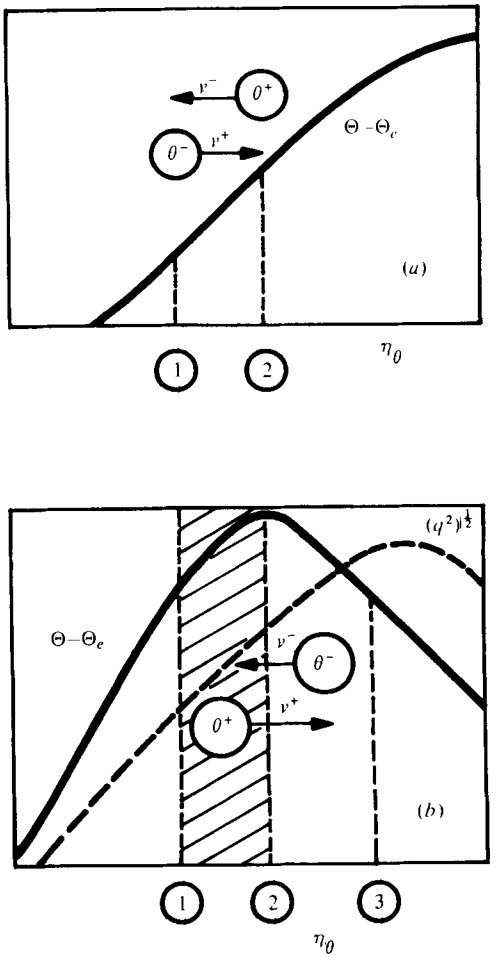

FIGURE 19. Turbulent bimodal structure of the dominant lateral fluxes. (*a*) Small-eddy motions. (*b*) Large-eddy motions in asymmetrical conditions.

can be explained only by large-scale exchanges between section 3, for example, where the mean temperature is lower than in the zone (1, 2), and a section located in the displacement zone. This preferential diffusion around the temperature maximum provides a lateral flux with opposite sign to the lateral gradient of the turbulence intensity. This result has been found previously in the equivalent dynamic case of the wall jet (Mathieu 1959) and the asymmetric plane jet (Béguier 1965*a*). However, in the asymmetric wake of Palmer & Keffer (1972) such behaviour was not observed.

In summary, we have shown that 'negative production' of temperature fluctuations can exist in an asymmetric mean thermal field of a classical turbulent shear flow. The situation is analogous to the 'negative production' of velocity fluctuations for the dynamic case in that large-eddy motion is required to explain the dominant transport processes. The results show that when an asymmetry exists the large eddies will convect fluid in a direction opposite to that of the gradient diffusion process of the small eddies, creating the zone of negative production. The bimodal or double-eddy model satisfactorily describes the phenomenon. It would be interesting to examine

the situation in which a coincident asymmetric velocity and thermal field exist. Such experiments are currently under way.

The work was carried out at I.M.S.T. in Marseille, a laboratory associated with C.N.R.S. Support for the study was provided as well by N.A.T.O. grant no. 956 and National Research Council of Canada grant A-2746. The authors would like to thank Dr R. Dumas for his help in this project and M. Astier for his technical contribution. Thanks are also expressed to Dr J. G. Kawall for his comments on the manuscript.

REFERENCES

BÉGUIER, C. 1965*a* *J. Méc.* **4**, 319.

BÉGUIER, C. 1965*b* *C. R. Acad. Sci. Paris* A **260**, 5460.

BÉGUIER, C. 1969 *C. R. Acad. Sci. Paris* A **268**, 69.

BÉGUIER, C. 1971 Thesis, Université de Provence, Marseille.

BÉGUIER, C., FULACHIER, L., KEFFER, J. F. & DUMAS, R. 1975 *C. R. Acad. Sci. Paris* B **280**, 493.

BÉGUIER, C., REY, C., DUMAS, R. & ASTIER, M. 1973 *C. R. Acad. Sci. Paris* A **277**, 475.

BRODKEY, R. S., NYCHAS, S. G., TARABA, J. L. & WALLACE, J. M. 1973 *Phys. Fluids* **16**, 2010.

BROWN, G. L. & ROSHKO, A. 1974 *J. Fluid Mech.* **64**, 775.

DAVIES, A. E., KEFFER, J. F. & BAINES, W. D. 1975 *Phys. Fluids* **18**, 770.

DEARDORFF, J. W. 1966 *J. Atmos. Sci.* **23**, 503.

DUMAS, R. 1964 *Publ. Sci. Tech. Minist. Air* no. 404.

DUMAS, R., FULACHIER, L. & ARZOUMANIAN, E. 1972 *C. R. Acad. Sci. Paris* A **274**, 267.

ERIAN, F. F. & ESKINAZI, S. 1964 *Univ. Syracuse, Res. I.N.S.T. Rep.* ME 937-6410 F.

ESKINAZI, S. & ERIAN, F. F. 1969 *Phys. Fluids* **12**, 1988.

ESKINAZI, S. & YEH, H. 1956 *J. Aero. Sci.* **23**, 23.

FAVRE, A. 1965 *J. Méc.* **4**, 361.

FAVRE, A. 1975 *Proc. 5th Can. Cong. Appl. Mech., Fredericton*, G-3.

FULACHIER, L., GIOVANANGELI, J. P., DUMAS, R., KOVASZNAY, L. S. G. & FAVRE, A. 1974*a* *C. R. Acad. Sci. Paris* A **278**, 683.

FULACHIER, L., GIOVANANGELI, J. P., DUMAS, R., KOVASZNAY, L. S. G. & FAVRE, A. 1974*b* *C. R. Acad. Sci. Paris* A **278**, 999.

FULACHIER, L. & DUMAS, R. 1976 *J. Fluid Mech.* **77**, 257.

GEE, M. T. & BRADSHAW, P. 1962 *Aero. Res. Counc. R. & M.* no. 3252.

GOSSE, J. & SCHIESTEL, R. 1975 *Int. J. Heat Mass Transfer* **18**, 743.

HANJALIĆ, K. & LAUNDER, B. E. 1971 *Imp. Coll. Rep.* BL-TN-B-41.

HINZE, J. O. 1970 *Dutch J. Appl. Sci. Res.* **22**, 163.

HINZE, J. O., SONNENBERG, R. E. & BUILTJES, P. J. H. 1974 *Appl. Sci. Res.* **29**, 1.

KEFFER, J. F., OLSEN, G. F. & KAWALL, J. G. 1977 *J. Fluid Mech.* **79**, 595.

KJELLSTRÖM, B. & HEDBERG, S. 1966 *Roy. Inst. Tech. Stockholm Rep.* AE 243.

LAUNDER, B. E. 1968 *Imp. Coll. Rep.* BL-TN-2.

LIEPMAN, H. W. & LAUFER, J. 1947 *N.A.C.A. Tech. Note* no. 1257.

MATHIEU, J. & TAILLAND, A. 1965 *C. R. Acad. Sci. Paris* A **261**, 2282.

PALMER, M. D. & KEFFER, J. F. 1972 *J. Fluid Mech.* **53**, 593.

SUNYACH, M. 1971 Thesis, Université de Lyon.

TOWNSEND, A. A. 1956 *The Structure of Turbulent Shear Flow*, chap. 5. Cambridge University Press.

VEROLLET, E. 1972 Thesis, Université de Provence, Marseille.

WILSON, D. J. 1974 *Phys. Fluids* **17**, 674.

WINANT, C. D. & BROWAND, F. K. 1974 *J. Fluid Mech.* **63**, 237.

WYGNANSKI, I. & FIEDLER, H. 1970 *J. Fluid Mech.* **41**, 327.

YULE, A. J. 1975 *J. Fluid Mech.* **72**, 481.